ELSEVIER

Contents lists available at ScienceDirect

Biosensors and Bioelectronics

journal homepage: www.elsevier.com/locate/bios





Microelectrode array membranes to simultaneously assess cardiac and neurological signals of xenopus laevis under chemical exposures and environmental changes

Xing Xia ^a, Manoj Vishwanath ^b, Jimmy Zhang ^c, Sadaf Sarafan ^a, Ramses Seferino Trigo Torres ^c, Tai Le ^c, Michael P.H. Lau ^d, Anh H. Nguyen ^{a,d}, Hung Cao ^{a,c,d,*}

- ^a Department of Electrical Engineering and Computer Science, UC Irvine, Irvine, CA, 92697, USA
- ^b Donald Bren School of Information and Computer Sciences, UC Irvine, CA, 92697, USA
- ^c Department of Biomedical Engineering, UC Irvine, Irvine, CA, 92697, USA
- d Sensoriis, Inc, Edmonds, WA, 98026, USA

ARTICLE INFO

Keywords: Xenopus laevis Simultaneous ECG and EEG Monitoring Drug toxicity screening Drug-induced epilepsy Environmental monitoring Microelectrode array

ABSTRACT

Simultaneous monitoring of electrocardiogram (ECG) and electroencephalogram (EEG) in studied animal models requires innovative engineering techniques that can capture minute physiological changes. However, this is often administered with a bulky and/or invasive system that may cause discomfort to animals and signal distortions. Here, we develop an integrated bioelectronic sensing system to provide simultaneous recordings of ECG and EEG in real-time for *Xenopus laevis*. The microelectrode array (MEA) membrane and the distinct anatomy of Xenopus offer noninvasive multi-modal electrophysiological monitoring with favorable spatial resolution. The system was validated under different environmental conditions, including drug exposure and temperature changes. Under the exposure of Pentylenetetrazol (PTZ), an epilepsy-inducing drug, clear ECG and EEG alterations, including frequent ictal and interictal EEG events, 30 dB average EEG amplitude elevations, abnormal ECG morphology, and heart rate changes, were observed. Furthermore, the ECG and EEG were monitored and analyzed under different temperatures. A decrease in relative power of delta band was observed when cold environment was brought about, in contrast to an increase in relative power of other higher frequency bands while the ECG remained stable. Overall, the real-time electrophysiology monitoring system using the Xenopus model holds potential for many applications in drug screening and remote environmental monitoring.

1. Introduction

Electrophysiology is a pragmatic approach to apprehending the status and perception of animals. Certain animals are exceptionally sensitive to environmental changes, such as chemical exposure or temperature, enabling their abilities to timely perceive and react to different circumstances; and this can be exploited for environmental monitoring. Although large mammalian models such as primates have excellent similarities in sizes and genetics to humans, they are not always the ideal choice due to high cost, slow reproduction rate, and ethical issues (Baumans, 2004; Denayer et al., 2014). For small mammalian models, other notable disparities are regarding their different cardiac electrophysiological activities from those of humans. For instance, their heart rate (HR) can be several hundred beats per minute (bpm) while the

respective value for humans is \sim 60–70 bpm, questioning their suitability for studying the changes in cardiac electrophysiology. All these call for an alternative model that can facilitate easier accessibility and reliable monitoring.

In recent years, some fish and amphibian models such as zebrafish and *Xenopus laevis (X. laevis)* have been explored, owing to their fecundity, cardiac physiological similarity to mammals, and the complexity of the circadian clock in relation to behavioral, sleep cycle, cellular and molecular responses (Rasar and Hammes, 2006). Researchers have made considerable progress on obtaining electrophysiological signals from zebrafish using flexible electrodes (Cao et al., 2014; Lee et al., 2020). As EEG and ECG are commonly acquired contralaterally for majority of animal models, simultaneous monitoring is often implemented separately using two systems. As a result, it is

^{*} Corresponding author. Electrical and Biomedical Engineering, University of California, Irvine, Irvine, CA, 92697, USA. *E-mail address:* hungcao@uci.edu (H. Cao).

demanding to reduce the device size and bring comfort to test subjects. The relatively small size and low signal intensity of zebrafish make it more challenging for stable and high-quality ECG and EEG simultaneous monitoring.

In contrast, *X. Laevis* possesses several unique advantages that facilitate non-invasive simultaneous monitoring of electrophysiological signals from both the brain and the heart. Foremost, anatomical features such as the location of the heart, the absence of ribs, and the special structure of the transverse process on vertebrae allows easier acquisition of the posterior ECG than the anterior ECG. Besides, the close heartbrain proximity of Xenopus and the flat and streamlined skull shape permit the acquisition of ipsilateral ECG and EEG signals by microelectrode array (MEA) on a single piece of flexible membrane. Furthermore, *X. laevis*' hairless and smooth skin alleviates the difficulties in obtaining low noise and stable biopotentials. These advantages provide the opportunity to minimize the device size without sacrificing comfort and signal quality, promoting the use of *Xenopus* as a potential model for drug screening and other studies.

Pentylenetetrazol (PTZ) is an antagonist of gamma-aminobutyric acid (GABA) on GABA receptors via the Tert Butylbicyclophosphorothioate site (Huang et al., 2001). The PTZ compound is typically used for screening potential novel antiepileptic drugs and has become an approved drug (Löscher, 2011). PTZ can penetrate through the plasma membrane, allowing to induce seizures via intracellular sites of action (Bloms-Funke et al., 1996). The EEG alterations caused by PTZ effects had been studied in zebrafish (Cho et al., 2017) and *X. laevis* tadpoles (Hewapathirane and Haas, 2009; Holmes, 2008). Both works reported detections of high amplitude spikes, the criteria for epileptic events. Careful immobilization and perfusion were needed during recordings as zebrafish and tadpoles cannot stay out of water for a long time. Thus, adult *X. laevis* hold obvious advantages.

Research has been conducted to investigate the relationship between brain signals and temperature. The human EEG changes at different atmospheric temperatures and relative humidity levels were examined (Zhu et al., 2020). Neuronal activities in anesthetized mice were also studied with rise in temperature (de Labra et al., 2021). These studies proved the correlation between brain activities and changes in environmental temperatures. Meanwhile, it demonstrated the use of EEG as a robust index for examining the effects of environmental changes. Ectotherms including amphibians cannot maintain their body temperature under different conditions like mammals, making them less tolerant and more vulnerable to temperature changes. This characteristic makes them an ideal model to investigate environmental variations.

In this work, we developed a MEA with gold electrodes on a flexible polyimide film to simultaneously record ECG and EEG in adult *X. laevis*. The acquired multichannel electrophysiological signals were amplified by a differential amplifier and digitized by an analog to digital converter (ADC) for further data analysis. Using our system, ECG and EEG were monitored under drug exposures and temperature variations. The system rapidly and accurately responded to phenotype changes, which offer potential and practicality to build compact wearable electrophysiology monitoring devices based on *X. laevis* for various biological studies and monitoring.

2. Materials and methods

2.1. Animals

All animal protocols were reviewed and approved by the Institutional Animal Care and Use Committee (IACUC) protocol (#AUP-21-066, University of California, Irvine). Xenopus were maintained in separated aquaria with 21 °C freshwater cycling. The aquaria were in a room with a 12 h:12 h light: dark cycle. 33 adult wild-type female Xenopus were used for this study. Due to the distinct differences in body sizes and weight between female and male *X. laevis* and the limited availability of male *X. laevis* in our facility, only female Xenopus were

utilized in the experiments. There should be no significant differences among male and female *X. laevis* subjects in terms of physiological structure for electrophysiological assessment.

2.2. Microelectrode array design and fabrication

To ensure biocompatibility and flexibility of the sensors for a uniform and secure contact with the skin of Xenopus, we fabricated the electrodes on polyimide films with various thicknesses ranging from 25 to 125 μm (Kapton, Dupont, Wilmington, DE, USA). The fabrication process is shown in Supplementary Fig. S1. First, a Au/Cr layer of 200/20 nm was deposited on the polyimide substrate. Conventional lithography and wet etching processes were used to pattern the four 50- μm -diameter circular electrodes. After the cleaning and post baking process, the traces of the electrodes were encapsulated by a layer of hardened photoresist (Shipley, 1827; MICROPOSIT).

In compliance with the brain structure of a Xenopus, we positioned the 4-channel EEG recording electrodes on the scalp above the right and left sides of the telencephalon and the mesencephalon (Fan et al., 2018) (Fig. 1A). The reference electrode was located above the center of the cerebellum. Three total lengths (25, 35, and 45 mm) of MEAs were designed to cater to different demands of flexibility. The ECG recording electrodes were integrated on the 35- and 45-mm membranes. The distance between the ECG electrode and the reference electrode was 20 mm, referring to the average heart-brain distance of Xenopus we measured. The ECG and EEG recording electrodes share a common reference electrode. The baseline noises in ECG caused by brain signals from cerebellum area can be filtered out by additional signal processing. The electrodes were traced to contact pads with a size of 2 mm \times 0.35 mm each to fit Flat Flexible Cable (FFC) connectors (5034800, Molex, Lisle, IL). A subsidiary printed circuit board (PCB) was designed to facilitate better connections between the electrodes and the cables leading to the subsequent signal collecting system. On the PCB, a FFC connector with a 0.5 mm pitch was routed to a 2 row, 2.54 mm female socket header connector. The flexible electrode membrane was easily inserted and locked into a FFC connector, and the signal transmitting cables were connected to the female sockets on PCB by male pin headers (Fig. 1B).

2.3. ECG and EEG signal acquisition

X. laevis were deeply anesthetized by immersion in a buffered solution of 1.5 g/L tricaine methane sulfonate (MS-222). The subjects were sufficiently anesthetized with the loss of toe pinch response. After anesthesia, the Xenopus were rested on a test bed made of polydimethylsiloxane (PDMS) and specially designed to possess a concave surface to fit the anatomical shape of Xenopus. Then, the MEA was placed dorsally based on the location of brain and heart and fixed by a manual micromanipulator (M3301, World precision instruments Inc., Sarasota, FL) to reduce vibrations. Due to the differential shrinkage of Xenopus skin and the Kapton membrane, the electrodes adhered to the skin automatically, resulting in a better electrical conductivity. During the recordings, the anesthetized Xenopus and accompanying devices were placed in a Faraday cage on a vibration-free table. The signals were amplified 10,000-fold by a differential amplifier (A-M Systems Inc. 1700 Differential Amplifier, Carlsberg, WA) and filtered between 1 and 500 Hz with a cut-off frequency of 60 Hz (notch). The filtered signals were then digitized at a sampling rate of 1000 Hz using a Data Acquisition Hardware (National Instruments USB-6251 DAQ device, Austin TX, and LabVIEW), and stored for further data analysis. The full system setup is sketched and shown in Fig. 1C.

2.4. Drug exposure

PTZ-induced epilepsy and anti-epileptic drug (valproic acid (VPA)) experiments were conducted to validate the system for drug exposure.

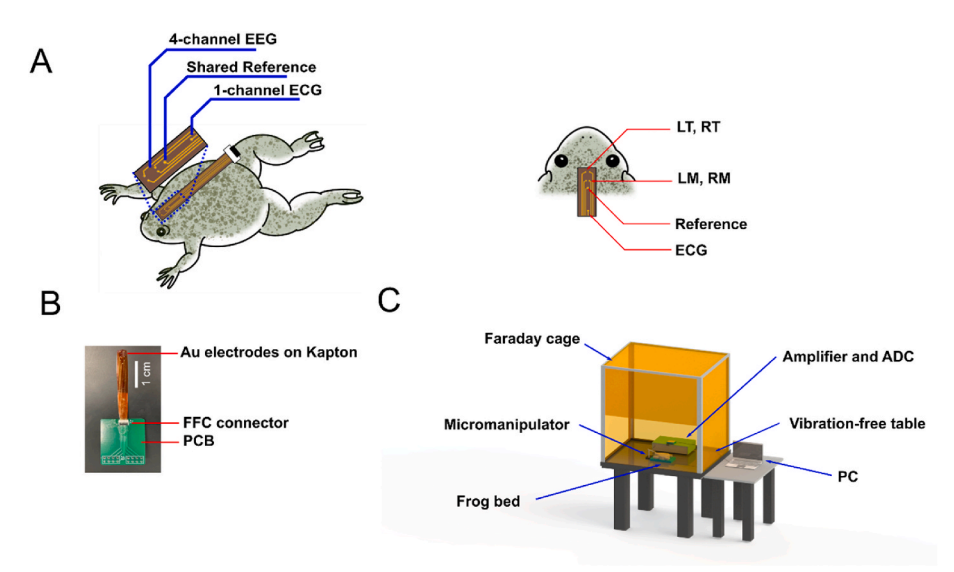


Fig. 1. The experimental setup and devices to record EEG and ECG simultaneously. A. 4 channel EEG and 1 channel ECG electrodes integrated on one polyimide membrane and the locations of electrodes, including left and right telencephalon (LT and RT) electrodes, left and right mesencephalon (LM and RM) electrodes, a reference electrode, and an ECG electrode. B. A picture of the microelectrode array and the PCB connector. C. The experimental setup includes a Faraday cage, a differential amplifier, an analog-to-digital converter, and a laptop for data acquisition.

Owing to the excellent absorbability of Xenopus skin, they were treated by direct immersion into drug solvent. The Xenopus were placed into a container filled with 200 mL drug solvent, with their eyes and noses above the solvent level. The drugs were transported passively. Compared to injection, this method took longer to be effective. Here, 30 mM PTZ dissolved in 1.5 g/L MS-222 was used for PTZ exposure. The Xenopus were immersed in PTZ solution for 15 min (min). For VPA treatments, the Xenopus were immersed in 3 mM VPA solution for 1 h. During the drug treatment, the containers were covered by lids to prevent Xenopus from escaping. After recordings, Xenopus were moved to a tank with flushing water to help them recover from anesthesia and drug effects. It took approximately 30 min for Xenopus to fully recover. The drug-treated Xenopus were separated and maintained in recirculating tanks for 7 days.

2.5. Temperature control

A set of temperature-dependent electrophysiology measurements were performed. After the Xenopus were fully anesthetized, 15-min recordings were taken with Xenopus immersed in MS-222 solution (21 $^{\circ}\text{C}$, 1.5 g/L). Then, the anesthesia solution was replaced with prechilled MS-222 solution (12 $^{\circ}\text{C}$, 1.5 g/L), introduced into the experimental setup gently without any electrode displacement. The recording was continued for 15 min while the temperature of the bath was continuously monitored using a digital aquarium thermometer. Once the recordings were accomplished, the Xenopus were allowed to recover in freshwater for 30 min at room temperature and transferred to a separate aquarium.

2.6. Data processing

For accurate detection of ECG characteristics, noise cancellation is critical. The lowpass filter and Savitzky-Golay finite impulse response (FIR) smoothing filter (SG filter) were used to suppress the powerline interference and remove the baseline wander. The baseline drifted due to respiration and could be normalized by using a lowpass filter. The SG filter proposed by Savitzky and Golay (1964) is based on local least-squares polynomial approximation; and it was demonstrated as one of the most popular noise cancellation and smoothing methods.

The obtained EEG signals were filtered using a 6th order Butterworth bandpass filter from 0.5 to 40 Hz, based on the frequency bands of interest, which includes delta (0.5–4 Hz), theta (4–8 Hz), alpha (8–12 Hz), beta (12–30 Hz) and gamma (>30 Hz). The Fourier transform (FFT) of the filtered signal was then calculated and visually compared between

different groups to analyze the difference in frequency compositions of the signals. For analyzing the temperature effects on EEG, similar procedures were performed. The power of EEG recording was calculated in the above-mentioned frequency bands and compared across the two temperature settings. Relative power of different frequency bands was analyzed using the formula

$$Relative \ band \ power = \frac{Power \ in \ specific \ frequency \ band}{Total \ power} \tag{1}$$

The above calculations were done using the bandpower function in MATLAB R2020b which uses a modified periodogram to determine the average power in a specific frequency range.

3. Result and discussion

3.1. Simultaneous xenopus EEG and ECG recording

4 channel EEG and 1 channel ECG signals were recorded from 24 Xenopus which were separately raised as 4 groups and examined under different drug exposures. Each recording lasted 20-40 min, depending on the duration that Xenopus were in deep anesthesia. It took approximately 12 min for Xenopus to be fully anesthetized in 1.5 g/L MS-222 solution. Whenever the Xenopus lost toe-pinch reactions, we transferred the anesthetized Xenopus from the anesthesia solution to the test bed. Settling down the Xenopus and adjusting the position of the MEA membrane took 2-3 min. After these procedures, experimenters stayed away from the experiment area to minimize the disturbances to the recordings. Three different lengths (25 mm, 35 mm, 45 mm) and 3 different thicknesses (25 μm , 75 μm , 125 μm) of the polyimide membrane were tested. The 75-μm thick, 25-mm long probe and the 125-μm thick, 35-mm and 45-mm long probes displayed the best performances. These probes had similar flexibility and strength to the skin of Xenopus, thus, the conformability and longevity were significantly stronger. In some of the recordings, the recorded EEG signals were noisy if the Xenopus scalp had too much mucus. We used paper towels to gently wipe the area before applying electrodes, the signal quality was greatly improved. All experiments were conducted in a Faraday cage on a vibration-free table, which contributed to obtain a favorable signal-tonoise ratio (SNR).

A typical recording of PTZ-treated Xenopus 4-channel EEG is shown in Fig. 2A. The signals were obtained from the electrodes placed near the left and right sides of the telencephalon (LT and RT) and the left and right sides of the mesencephalon (LM and RM). This segment of recording included 20 s (sec) of normal EEG (baseline) followed by 20 s

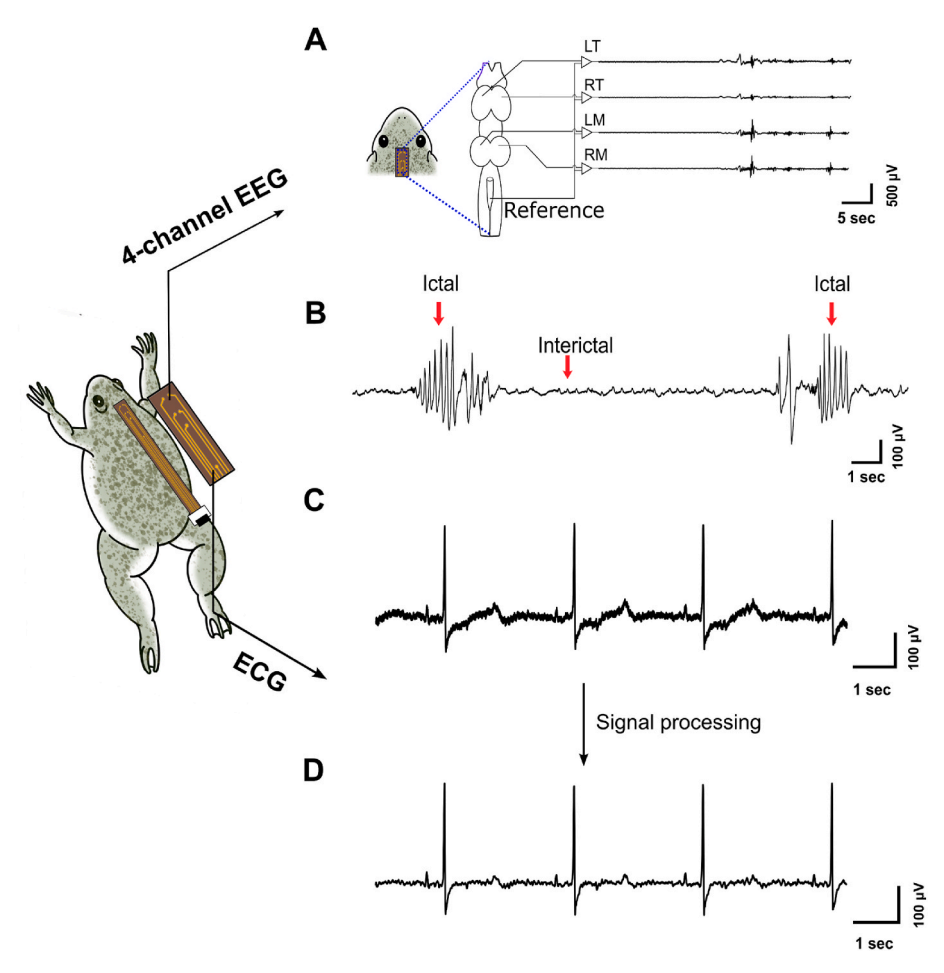


Fig. 2. Typical EEG signals recorded by system. A. 4 channel EEG from different locations of the brain in 40 sec. B. Typical EEG patterns of a seizure, includes two ictal events and one interictal period. C. Sample of 1 channel ECG recorded by the integrated ECG electrode. D. ECG after signal processing.

of the EEG during seizures of epilepsy. Periodic sharp spikes with much higher amplitude than the baseline EEG were observed and defined as the criteria for ictal seizures. Fig. 2B demonstrates the typical patterns of EEG before and after each epileptic seizure. There were periods of signals that had much higher amplitude spikes than regular EEG. We identified these periodic spikes with 200–600 μV high amplitudes as an ictal event. In the 20 s of recording, there were two ictal events. The high amplitude spikes in ictal events appeared 3-5 times in 1 s, and each ictal event contains 5-10 occurrences of such spikes, consistent through the whole recording. Between the two ictal events, some periodic bumps with lower amplitude and less sharpness were detected less frequently. These bumps were identified as an interictal event. The interictal events only appeared after the first appearance of the ictal event, and they disappeared before the ictal events ended. The small spikes of interictal intervals were around 40 µV, occurring 1-2 times in 1 s. The ictal and interictal events were not detected in the control group as the absence of focal epilepsy. In addition, a closer look of the 4 channel EEG during seizure events is shown in Supplementary Fig. S2. The EEG obtained from different locations had different patterns and amplitudes, which indicated the rough origins of epileptic neural activities.

Simultaneous ECG signals were recorded by the working electrodes that were dorsally placed close to the heart. Thanks to the short heart-brain distance of Xenopus, ECG recording electrode was closed to the 4-channel EEG electrodes, decreasing the size of the MEA membrane to less than 2 cm \times 0.5 cm while maintaining high-quality ECG and EEG recordings. We also chose to use the same ECG/EEG reference electrode which was placed on the cerebellum of Xenopus to further minimize the size of the device and maximize the comfort the animals while

monitoring. Despite obtaining mixed ECG and EEG signals from the same channel, the recorded ECG signals were good enough to be used for morphological analysis. Fig. 2C shows an example of a segment of the raw signals recorded by the ECG electrodes. The R peaks had amplitudes around 250 μV , which were much higher compared with the baseline noises (less than 20 μV). The R peaks were definable without additional filtering; hence the HR and R-R intervals could be extracted from the raw signals manually. We also tried to record the ECG with an individual ECG reference electrode placed on the right leg of Xenopus. While it provided better ECG signals, the trade-off between the total size and the signal qualities made it less ideal. Fig. 2D shows the ECG signals after noise cancellation and smoothing filtering. After data processing, the PORST waves were clear and definable.

Before we decided the placement of the electrodes, we tested ECG electrodes on different locations and compared the signal quality. As shown in Supplementary Fig. S3, the unique location of Xenopus heart and relative dorsolateral derma plica enabled the recording of ECG signals dorsally without losing important ECG information. This finding compelled us to implement the ipsilateral ECG and EEG recordings. Meanwhile, Xenopus' unique neck structure not only flattens their dorsum but also significantly decreases the distance between the heart and the brain. These characteristics of Xenopus came together and allowed simultaneous ECG and EEG recordings by electrodes fabricated on a small single piece of flexible substrate, which offered the opportunity to further minimize the device size. These findings strongly attest to the natural benefit of using Xenopus as the model for ECG and EEG simultaneous monitoring. We also compared ECG signals recorded using the same data acquisition system from human, zebrafish, and Xenopus as

shown in Supplementary Fig. 4.

The advancement of fabrication technology and electrical engineering in recent years have paved way for development of high spatial resolution EEG and ECG monitoring devices. Rats and mice were some of the most popular lab animal models. Many researchers presented wired or wireless multichannel rodent EEG recording devices (Choi et al., 2010; Pinnell et al., 2016). Some works also included a simultaneous ECG (Mishra et al., 2018). ECG and EEG recordings on zebrafish were realized as well but integrating them is still challenging. Most electrophysiology recording systems for small animal models were based on rodents or zebrafish. The other animal models were lack of exploration. In our work, we presented the feasibility of electrophysiology recording on Xenopus as a great alternative option. It has huge potentials in many applications owing to certain unique advantages.

3.2. PTZ-induced seizures and VPA anti-epileptic effects

The ECG and EEG signals were recorded and analyzed from 4 groups of Xenopus. 24 Xenopus were divided with different drug treatment conditions: (1) PTZ group, in which the Xenopus were treated in 200 mL solution with 30 mM PTZ mixed with 1.5 g/L MS-222; (2) VPA + PTZ group, in which they were immersed in 5 mM VPA solution for 1 h before they were transferred to the same PTZ treatment as the PTZ group; (3) VPA group, in which Xenopus were treated with 5 mM VPA for 1 h then transfer to MS-222 solution; and (4) Control group, where no drug treatment was administered before anesthesia. Each Xenopus was anesthetized in 1.5 g/L MS-222 then recorded for more than 25 min.

The typical 1500-s-long recordings of raw EEG signals from the control group, PTZ group and the VPA + PTZ group are demonstrated in Fig. 3A-C, respectively. The 1500-s-long samples were recorded by the LT working electrodes (channel 1), the other 3 EEG channels showed similar results statistically, as all channels were able to record the same number of ictal events. The obtained signals of the experimental groups were recognizably different in the occurrences and the amplitudes of PTZ-induced seizures. EEG recorded in the control group did not show any occurrence of seizures. The average amplitude of the control group

EEG was 10 μV. In the PTZ group and the VPA + PTZ group, the ictal event occurrence, previously identified by spikes in amplitudes of $200-600 \mu V$, was 34 times and 2 times, respectively. However, upon a closer look into the EEG patterns in the VPA + PTZ group, we found the average amplitudes of the ictal spikes decreased 81.0% from $370~\mu V$ to $70 \mu V$. In consideration of this factor, the criteria of an ictal event for VPA + PTZ group was changed to $37.8-113.5 \mu V$, proportional to the decrease in amplitudes of spikes. After recalculation, the ictal events in the VPA + PTZ group in the 1500-s-long recording appeared 9 times, resulting in a 73.5% reduction in comparison with the PTZ group subjects. These results proved that VPA can mitigate PTZ-induced seizures in terms of occurrences and intensities, which is in accordance with studies on other models (Puig-Lagunes et al., 2016; Romoli et al., 2019). The recordings obtained from different groups also validate our device for its capability and longevity to collect high SNR EEG for long-term monitoring.

The Fast Fourier Transform (FFT) spectrums averaged across 4 recorded channels of the 4 groups are shown in Fig. 3D. It quantified the number of different frequency components present in the given signal. In general, all 4 groups had higher amplitudes in low frequencies, which is a characteristic for all EEG signals. It is observable that the amplitude of the PTZ group was 30 dB higher than the control group and the VPA group for the entire frequency range of frequencies (0-50 Hz). The averaged amplitude of EEG signals in 4 groups was also calculated and compared as shown in Fig. 3E. The error bars were standard deviation values calculated from 4 separate groups. The Control group and the VPA group did not have noticeable differences, indicating that the VPA did not cause significant EEG changes in the frequency domain. With the exposure of PTZ, the average EEG amplitude increased 833.9% compared with that in the control group. In the VPA treated groups, the amplitude increased 70.0% after the immersion of PTZ, resulting in a 91.6% mitigation of PTZ effects. The averaged amplitude in the control group and VPA treated group did not show significant differences, which indicated that the VPA did not have mitigation effects on non-seizure EEG amplitude.

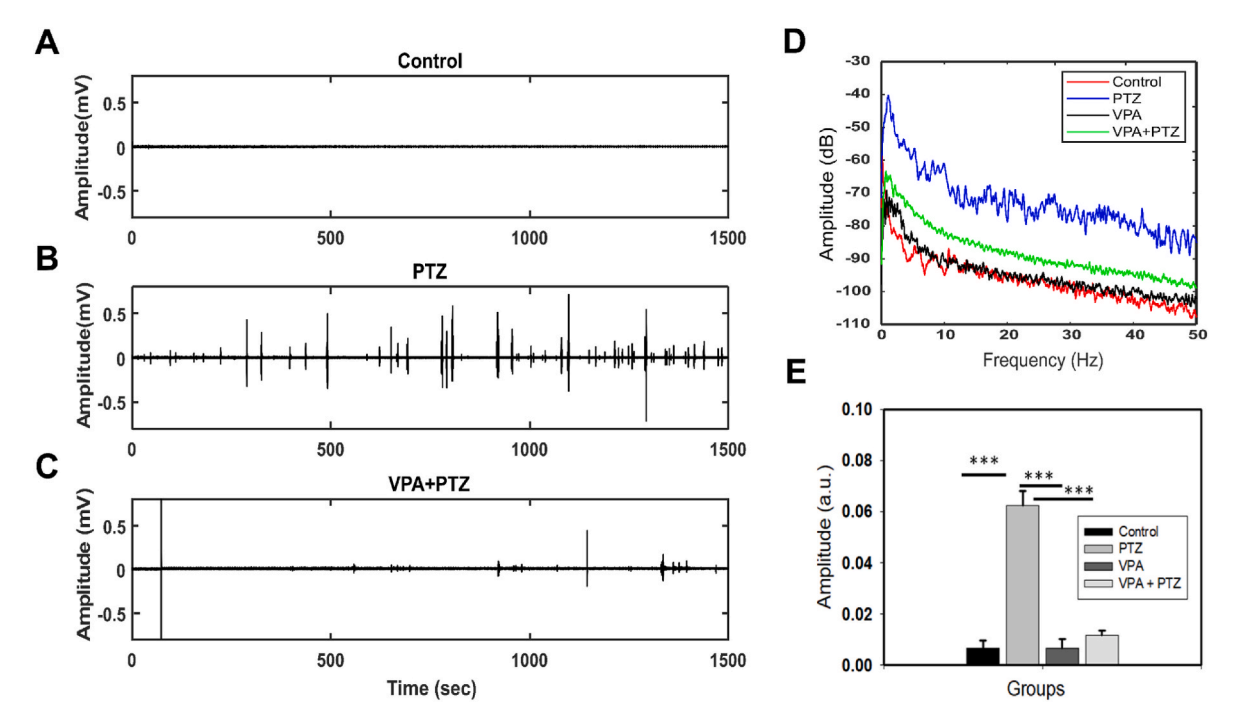


Fig. 3. PTZ and VPA effects to Xenopus EEG. A. 1500 s EEG of Xenopus in control group; B. in PTZ group; C. in VPA + PTZ group. D. Fast Fourier transform of the EEG in 4 groups. The groups treated with PTZ showed higher amplitude in 0–40 Hz frequency domain, but the VPA inhibited the PTZ effects. E. The average amplitude of EEG in 4 groups for quantified comparisons.

3.3. Epilepsy-induced cardiac rhythm disorder

ECG changes caused by drug exposures were also observed. In our experiments, the HR, R-R intervals, QTc intervals and morphological characteristics of Xenopus ECG were analyzed. The average HR was calculated at an interval of every 2 min for each Xenopus after the PTZ treatment. Since the HR of Xenopus differed widely in certain individuals (from 11 bpm to 52 bpm in our dataset), the relative heart rate (RHR), which is the HR at one moment in time divided by the averaged HR of the whole recording, was used to represent the HR variation. The average RHR variation of the 6 Xenopus after the treatment of PTZ were shown in Fig. 4A. The purple line represented the average RHR trend; the error bars were the highest and lowest RHR at the time points in the PTZ group. The first appearances of epileptic seizures were determined from the simultaneously recorded EEG signals. The first appearance of an ictal event in the EEG signals was defined as the boundary between the preictal stage and the ictal stage (Fisher et al., 2014). The boundaries appeared at around 10 min into the ECG recordings. The 2 stages were marked with different colors in the figure. By investigating the trends of the Xenopus HR variation in PTZ group, we found that the RHR did not increase when seizures occurred. On the contrary, the HR was even lower in the Ictal stage than the Preictal stage for all the Xenopus tested. To compare the effects of anesthesia on HR, control group consisting of Xenopus that were only treated with MS-222 at the same concentration and duration as other experimental groups was introduced. Fig. 4B showed the RHR variation in 30-min-long recordings of the control group. The blue line was the trend of RHR of the control group, with error bars marked as the maximum and minimum values of each data point. The RHR curve of the PTZ group was shown as the red dotted line for comparison. Both groups had very similar HR variation from the 10th to 30th min of the recording, which was defined as the Ictal stage in the PTZ group. But the RHR variation in the Preictal stage of the control group was more moderate. This comparison indicated that the PTZ has caused increases in HR, but it gradually returned to normal. Additionally, when the ictal events were detected in EEG signals, which indicated the occurrence of epileptic seizures, the HR did not increase.

PTZ also induced morphological changes on the ECG patterns. The ECG morphology changes were not identical across all Xenopus. From the PTZ group, one Xenopus was found to possess gradually inverted T waves during the recording. The ECG after PTZ treatment was shown in Fig. 5A. Four intervals of ECG were selected, which are (a), the start of the recording; (b), the end of the preictal period; (c), the start of the ictal events; and (d), the end of the recording. From (a) to (d), the R-R intervals increased from 1.7 s to 4.7 s, and the T waves changed from upright in (a) and (b), to flat in (c), and then inverted in (d). As the figure depicts, the morphology of other waves did not have significant change

besides T waves. Another Xenopus was detected to have 3 min of arrhythmia when seizures occurred. The ECG is shown in Fig. 5B. The arrhythmia happened right after the occurrence of the first ictal event. Before and after this 3-min interval of arrhythmia, the R-R interval was around 2.8 s. When the arrythmia occurred, the heart beats were in pairs as one fast heart rhythm and one slow rhythm. The R-R intervals were 1.6 s and 2.7 s, respectively. In contrast, the morphology of ECG did not have noticeable changes for all subjects in the control group.

3.4. Temperature-dependent EEG-ECG features

Considering the temperature tolerance range of Xenopus laevis (McNamara et al., 2018), the environmental temperature was controlled within 12 °C-21 °C.The experiments were conducted following the timeline shown in Fig. 6A. The change in temperature and RHR during the experiment is shown in Fig. 6B. As seen, the temperature before the introduction of cold MS-222 solution stayed stable, afterwards, while the temperature of cold tricaine rises following a quasi-logarithmic curve. The HR changes were extracted from the ECG signals. We calculated the average RHR of 4 Xenopus and the curve is shown as the red dotted line. The RHR increased slightly from 0.95 to 1.08, which is much less significant than the PTZ results. The effects of cold temperature on the relative band power of different EEG bands can be clearly seen in Fig. 6C-F. For Delta band, the relative power stayed stable before the temperature dropped. Once the cold MS-222 solution was introduced, the relative band power decreased 7.0% on average, then gradually increased from 62.1% to 72.3% in the subsequent 700 s, while the HR stayed stable during the whole measurement. The more distinct changes were found in Alpha band, as presented in Fig. 6D. The relative power increased 59.4%, from 3.7% to 5.9%, during the changing of cold MS-222 solution. After the introduction of cold solution, the Alpha relative band power dropped from 5.9% to 4.4%, in 700 s. The Theta and Beta relative band power shows similar trends as the Alpha band (Fig. 6E and F). Overall, the Alpha band relative power had the most significant variation while the temperature changing. The high frequency signals increased then gradually dropped to normal level during the time Xenopus stayed in cold environments, while the low frequency signals in Delta band, showed reversal of trend.

Amphibians are particularly sensitive to changes in climatic conditions due to various factors such as physiological process and temperature and moisture-dependent breeding patterns. Due to limited dispersal capacity, change in external climatic conditions may pave the way to slight differences in evolution among its different population groups. In conjunction with the fact that Xenopus is one of the most widely distributed amphibians found in four continents (North America, South America, Europe, and Asia), and climate change in all likelihood

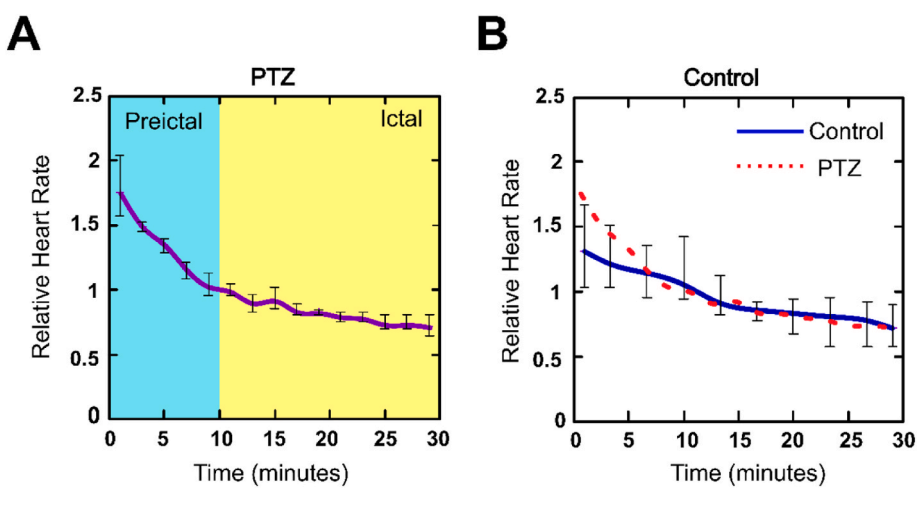


Fig. 4. Relative heart rate altering. A. The RHR changings during the 30 min recordings in PTZ group. B. The comparison of RHR trends in PTZ and Control group.

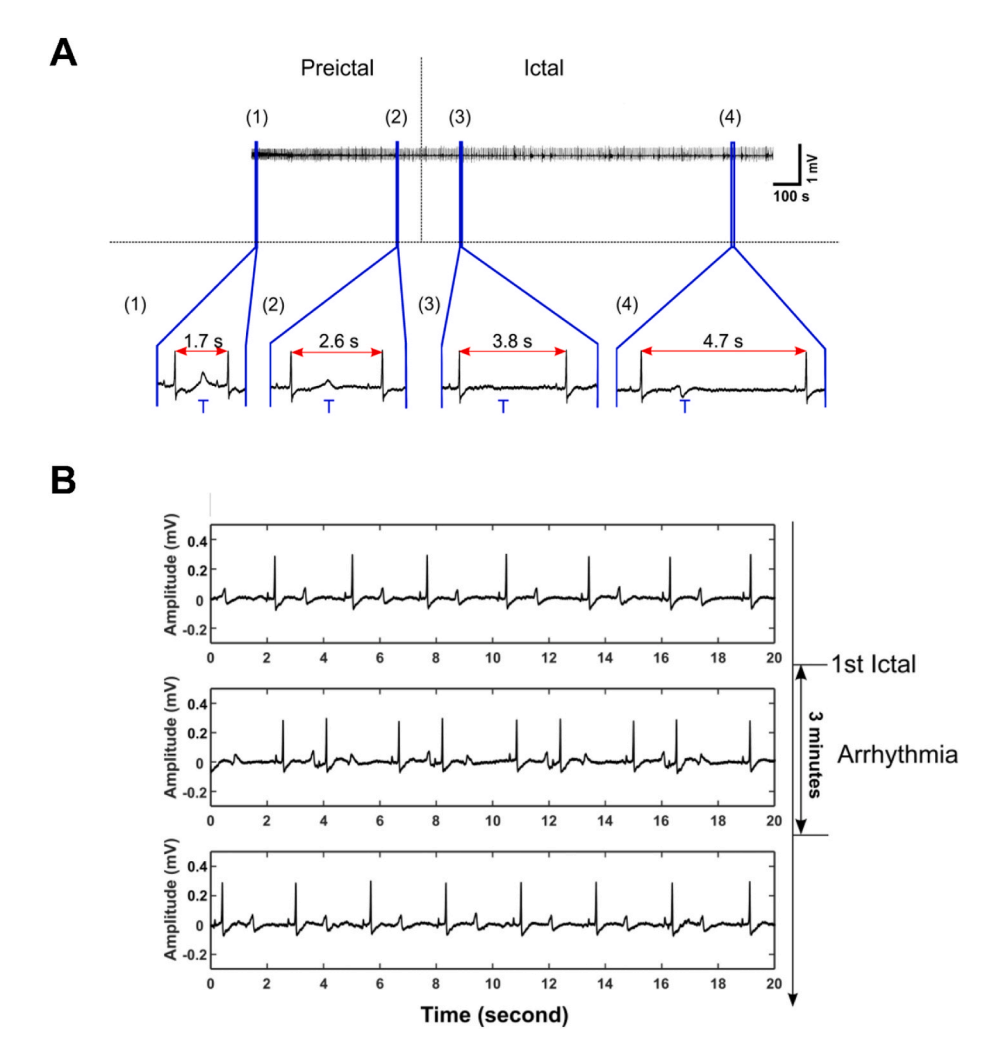


Fig. 5. Abnormal ECG found in PTZ-treated Xenopus. A. T wave gradual inversion in a 30-min recording. B. 3-Min arrhythmia happened right when ictal events started.

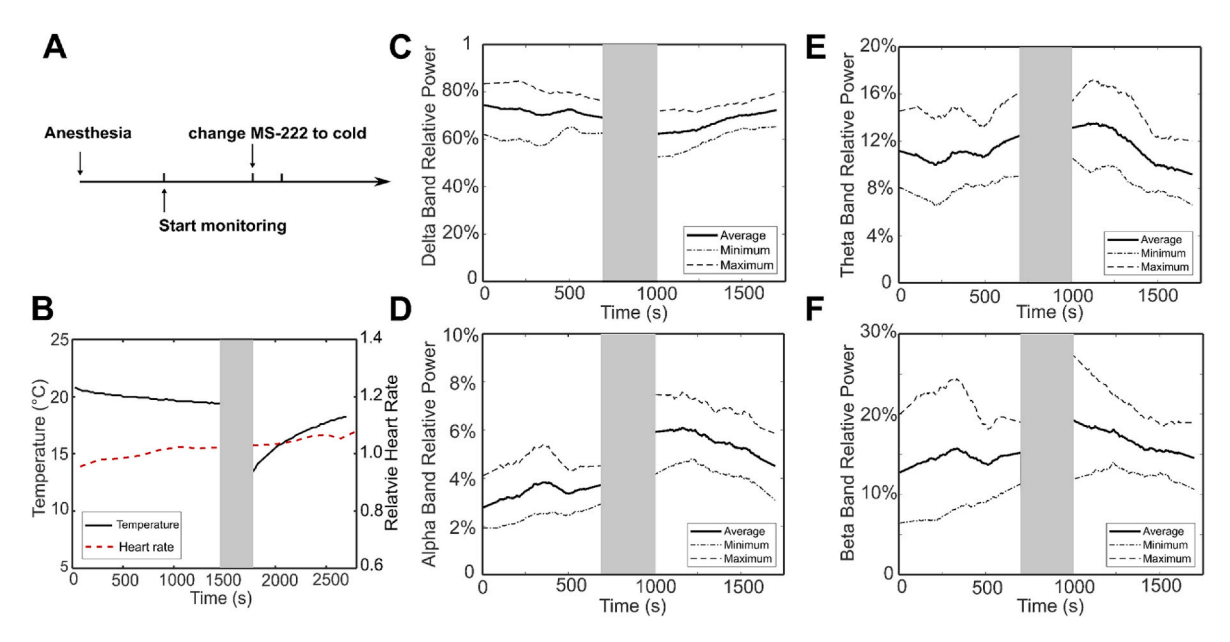


Fig. 6. Temperature dependent EEG features A. Monitoring protocol while the temperature changed without major disturbances to recordings. B. Environment temperature and RHR during the recording session. C. Relative band power trends of the recorded EEG signals, including the average, maximum and minimum relative band power of the samples in Delta wave band, D. in Alpha wave band, E. in Theta wave band and F. in Beta wave band.

increasing the invasion potential and population growth of Xenopus (Ihlow et al., 2016). Its use as a model organism to study the change in environmental conditions globally is crucial. It is worth mentioning that another well-known species of Xenopus, *Xenopus tropicalis*, prefers warmer waters at temperature of 24–26 °C, which is 5–7 °C higher than the living water temperature of *X. laevis* (Blum and Ott, 2018). Since the two species share many common characteristics in body structures, the similar recording system can be applied to Xenopus tropicalis, especially when higher environmental temperature is of interest.

4. Conclusion and future work

In this work, a multichannel ECG-EEG recording system on Xenopus was developed. Although, X. laevis has not been widely used for studies involving electrophysiological monitoring, we discovered great potential in using this animal model for environmental monitoring and drug screening. The flexible MEA membrane placed dorsally on Xenopus noninvasively recorded the ECG and EEG simultaneously when the frogs were under anesthesia. The sensor is compact and easy to setup. The PTZ and VPA drug tests and the temperature control test validated the feasibility of this system in real time monitoring of ECG and EEG for associated neurological and cardiovascular conditions. Both signals displayed detectable and distinct characteristics during different stages of seizures. With excellent skin permeability and easy-to-obtain electrophysiological signals, Xenopus could serve as a desired model for sensing and monitoring of chemical exposure and environmental changes. Future work includes the development of a miniaturized system on a more flexible substrate, such as parylene C, with embedded microelectronics and wireless communication, so that awake electrophysiology signals can be monitored without interferences from Xenopus behavior.

CRediT authorship contribution statement

Xing Xia: Conceptualization, Data curation, Formal analysis, Investigation, Methodology, Writing – original draft, Writing – review & editing. Manoj Vishwanath: Data curation, Formal analysis, Investigation, Writing – review & editing. Jimmy Zhang: Data curation, Methodology. Sadaf Sarafan: Formal analysis, Writing – review & editing. Ramses Seferino Trigo Torres: Data curation, Methodology. Tai Le: Data curation, Methodology. Michael P.H. Lau: Writing – review & editing. Anh H. Nguyen: Conceptualization, Formal analysis, Investigation, Methodology, Writing – original draft, Writing – review & editing. Hung Cao: Conceptualization, Writing – original draft, Writing – review & editing.

Declaration of competing interest

The authors declare that they have no known competing financial interests or personal relationships that could have appeared to influence the work reported in this paper.

Acknowledgement

The authors would like to acknowledge the financial support from the NSF CAREER Award #1917105 (H.C.), the NSF #1936519 (H.C.), and the NIH SBIR grant #R44OD024874 (M.P.H.L and H.C.). We thank Lauren Schmiess-Heine and Roger Geertsema for managing the Xenopus facility.

Appendix A. Supplementary data

Supplementary data to this article can be found online at https://doi.org/10.1016/j.bios.2022.114292.

References

- Baumans, V., 2004. Use of animals in experimental research: an ethical dilemma? Gene Ther. 11 (1), S64–S66.
- Bloms-Funke, P., Madeja, M., Muβhoff, U., Speckmann, E.J., 1996. Effects of pentylenetetrazol on GABA receptors expressed in oocytes of Xenopus laevis: extraand intracellular sites of action. Neurosci. Lett. 205 (2), 115–118.
- Blum, M., Ott, T., 2018. *Xenopus*: an undervalued model organism to study and model human genetic disease. Cells Tissues Organs 205 (5–6), 303–313.
- Cao, H., Yu, F., Zhao, Y., Zhang, X., Tai, J., Lee, J., Darehzereshki, A., Bersohn, M., Lien, C.-L., Chi, N.C., Tai, Y.-C., Hsiai, T.K., 2014. Wearable multi-channel microelectrode membranes for elucidating electrophysiological phenotypes of injured myocardium. Integr Biol (Camb) 6 (8), 789–795.
- Cho, S.-J., Byun, D., Nam, T.-S., Choi, S.-Y., Lee, B.-G., Kim, M.-K., Kim, S., 2017. Zebrafish as an animal model in epilepsy studies with multichannel EEG recordings. Sci. Rep. 7 (1), 3099.
- Choi, J.H., Koch, K.P., Poppendieck, W., Lee, M., Shin, H.-S., 2010. High resolution electroencephalography in freely moving mice. J. Neurophysiol. 104 (3), 1825–1834
- de Labra, C., Pardo-Vazquez, J.L., Cudeiro, J., Rivadulla, C., 2021. Hyperthermiainduced changes in EEG of anesthetized mice subjected to passive heat exposure. Front. Syst. Neurosci. 15.
- Denayer, T., Stöhr, T., Van Roy, M., 2014. Animal models in translational medicine: validation and prediction. New Horizons in Translational Medicine 2 (1), 5–11.
- Fan, Y., Yue, X., Xue, F., Brauth, S.E., Tang, Y., Fang, G., 2018. The right thalamus may play an important role in anesthesia-awakening regulation in frogs. PeerJ 6 e4516e4516.
- Fisher, R.S., Scharfman, H.E., deCurtis, M., 2014. How can we identify ictal and interictal abnormal activity? In: Scharfman, H.E., Buckmaster, P.S. (Eds.), Issues in Clinical Epileptology: A View from the Bench. Springer Netherlands. Dordrecht, pp. 3–23.
- Hewapathirane, D.S., Haas, K., 2009. The albino Xenopus laevis tadpole as a novel model of developmental seizures. In: Baraban, S.C. (Ed.), Animal Models of Epilepsy: Methods and Innovations. Humana Press, Totowa, NJ, pp. 45–57.
- Holmes, G.L., 2008. Commentary on Hewapathirane et al. (in vivo imaging of seizure activity in a novel developmental seizure model) seizure-induced brain damage: from tadpoles to children. Exp. Neurol. 213 (1), 7–9.
- Huang, R.-Q., Bell-Horner, C.L., Dibas, M.I., Covey, D.F., Drewe, J.A., Dillon, G.H., 2001. Pentylenetetrazole-induced inhibition of recombinant γ -aminobutyric acid type A (GABA_A) receptors: mechanism and site of action. J. Pharmacol. Exp. Therapeut. 298 (3), 986–995.
- Ihlow, F., Courant, J., Secondi, J., Herrel, A., Rebelo, R., Measey, G.J., Lillo, F., De Villiers, F.A., Vogt, S., De Busschere, C., Backeljau, T., Rödder, D., 2016. Impacts of climate change on the global invasion potential of the african clawed frog Xenopus laevis. PLoS One 11 (6), e0154869.
- Lee, Y., Lee, K.J., Jang, J.-W., Lee, S.-i., Kim, S., 2020. An EEG system to detect brain signals from multiple adult zebrafish. Biosens. Bioelectron. 164, 112315.
- Löscher, W., 2011. Critical review of current animal models of seizures and epilepsy used in the discovery and development of new antiepileptic drugs. Seizure 20 (5), 359–368
- McNamara, S., Wlizla, M., Horb, M.E., 2018. Husbandry, general Care, and transportation of Xenopus laevis and Xenopus tropicalis. In: Vleminckx, K. (Ed.), Xenopus: Methods and Protocols. Springer New York, New York, NY, pp. 1–17.
- Mishra, V., Gautier, N.M., Glasscock, E., 2018. Simultaneous video-EEG-ECG monitoring to identify neurocardiac dysfunction in mouse models of epilepsy. JoVE 131, e57300.
- Pinnell, R.C., Almajidy, R.K., Kirch, R.D., Cassel, J.C., Hofmann, U.G., 2016. A wireless EEG recording method for rat use inside the water maze. PLoS One 11 (2) e0147730e0147730.
- Puig-Lagunes, A.A., Manzo, J., Beltrán-Parrazal, L., Morgado-Valle, C., Toledo-Cárdenas, R., López-Meraz, M.-L., 2016. Pentylenetetrazole-induced seizures in developing rats prenatally exposed to valproic acid. PeerJ 4 e2709-e2709.
- Rasar, M.A., Hammes, S.R., 2006. The physiology of the Xenopus laevis ovary. In: Liu, X. J. (Ed.), Xenopus Protocols: Cell Biology and Signal Transduction. Humana Press, Totowa, NJ, pp. 17–30.
- Romoli, M., Mazzocchetti, P., D'Alonzo, R., Siliquini, S., Rinaldi, V.E., Verrotti, A., Calabresi, P., Costa, C., 2019. Valproic acid and epilepsy: from molecular mechanisms to clinical evidences. Curr. Neuropharmacol. 17 (10), 926–946.
- Savitzky, A., Golay, M.J.E., 1964. Smoothing and differentiation of data by simplified least squares procedures. Anal. Chem. 36 (8), 1627–1639.
- Zhu, M., Liu, W., Wargocki, P., 2020. Changes in EEG signals during the cognitive activity at varying air temperature and relative humidity. J. Expo. Sci. Environ. Epidemiol. 30 (2), 285–298.